Zeeman Splitting in Pd and Pt Calculated from Self-Consistent Band Structure Including an External Magnetic Field

Anders Hjelm
Department of Technology, Uppsala University, Box 534, S-751 21 Uppsala, Sweden

Jean-Louis Calais
Department of Quantum Chemistry, Uppsala University, Box 518, S-751 20 Uppsala, Sweden
(Received 30 May 1991)

Fully self-consistent band-structure calculations have been performed for palladium and platinum. The effective Hamiltonian contains exchange, correlation, and relativistic effects as well as the external magnetic field. The anisotropy of the cyclotron-orbit Zeeman splitting agrees well with experimental data from de Haas–van Alphen measurements. The calculated total susceptibilities also agree with the experimental values.

PACS numbers: 71.70.Ej, 71.25.Jd, 75.20.En

The Zeeman splitting of cyclotron orbits has been thoroughly investigated by means of the de Haas–van Alphen (dHvA) effect. In the alkali metals [1] the Zeeman splitting is found to be isotropic, but the g factor deviates from the free-electron value of 2. On the other hand, in Rh [2], Pd [3,4], Ir [5], and Pt [6,7] the cyclotron-orbit g factor (g_c) is found to be strongly anisotropic, and it is also known that in Pd and Pt the average g factor is large. The g_c factor in the noble metals [8] also shows a strong anisotropy. Previous experience indicates that simple band-structure models with the magnetic field taken into account by first-order perturbation theory cannot explain this behavior.

To our knowledge, no calculations aiming at a total picture of the Zeeman splitting have been performed. MacDonald [9] has calculated average g factors for the transition metals including spin-orbit coupling, but without exchange and correlation effects. Jarlborg and Freeman [10] have calculated g factors for certain **k** points on the Fermi surface of Pd, neglecting spin-orbit coupling. For comparison with dHvA experiments, cyclotron-orbit values must be calculated. This has been done, including spin-orbit coupling but without enhancement of the Zeeman splitting from exchange and correlation, for the platinum group metals [11], noble metals [12], and alkali metals [13]. These studies show that spin-orbit coupling is the dominant source of the anisotropy for most Fermi-surface sheets and indicate that exchange and correlation enhancement must be included in the model in order to also get the right order of magnitude of the Zeeman splitting. In the present paper results for Pd and Pt are presented using a calculational scheme where the external magnetic field is included in the self-consistent cycle, which allows the spin-dependent exchange-correlation potential and the spin-orbit coupling to affect the Zeeman splitting.

In an external magnetic field, a Fermi-surface sheet in a paramagnetic or diamagnetic metal is split into two slightly different surfaces. The interference between the two dHvA signals of these sheets will then appear as a modulation of the amplitude, according to a cosine function with argument πR, where

$$R=\frac{\hbar}{2\pi e}\frac{A_1-A_2}{B}, \tag{1}$$

A_1 and A_2 are the extremal cross-sectional areas of the two split surfaces perpendicular to the magnetic field, and B is the applied field strength. In moderate fields (i.e., for small splittings) R can be approximated by

$$R=g_c m_c/2, \tag{2}$$

where m_c is the effective cyclotron mass in units of the free-electron mass. In this paper, R is calculated and compared to experimental data, as it is unaffected by electron-phonon effects [14], in contrast to g_c where the uncertainty of the electron-phonon coupling parameter makes comparisons more difficult.

The spin-polarized, self-consistent band structures were calculated using the method of linear muffin-tin orbitals with atomic-sphere approximation (LMTO-ASA) [15] and the local-spin-density approximation (LSDA). The canonical structure constants and combined correction terms were calculated in a coordinate system with the z axis parallel to the direction of the magnetic field. As the point-group symmetry is reduced when a field is applied in an arbitrary direction the **k** points must be sampled over at least half the Brillouin zone (BZ). Because of spin-orbit coupling, the amount of m_l character in the wave functions varies from one-half of the BZ to the other. As this affects the orbital magnetic moment it turned out that integration over the entire BZ was necessary in order to get the accuracy needed. The number of **k** points used was 17 632, corresponding to a density of 505 **k** points per $\frac{1}{48}$ of the BZ. The band Hamiltonian contained a kinetic-potential term as described in Ref. [15], a spin-orbit term, and a Zeeman term $[\mu_B \mathbf{B}\cdot(\boldsymbol{l}+2\mathbf{s})]$. A derivation of the matrix elements of the two latter operators will be given elsewhere.

In order to calculate a new potential for the band Hamiltonian the spherically averaged charge and spin distributions, constructed from the total and m_l- and spin-projected state densities, were used together with the frozen-core charge distribution and the spin-dependent exchange-correlation potential according to von Barth and Hedin [16]. To this end, the Dirac equation without spin-orbit coupling was solved, thus including the mass velocity and Darwin shifts. This way of treating relativistic effects is often referred to as the scalar relativistic approximation [17].

This procedure was iterated until self-consistency was achieved for each field direction and each field strength. The convergence criteria were that the center of gravity of each m_l- and spin-projected band should not differ by more than 15 μRy, and that the average of all differences should not be larger than 10 μRy, between two successive iterations. In a field of 10 T the smaller amount of energy corresponds to a change in g factor of 0.2. Angular momenta larger than 2 were neglected, in order to save computing time. However, preliminary calculations including f orbitals show that the occupancy of the f states is less than 0.2 electron per atom, and the anisotropic behavior is affected very little. A small increase in the total susceptibility is also noticed.

The self-consistent band Hamiltonian was then used to calculate the split extremal cross-sectional Fermi-surface areas, by varying the length of the $\mathbf{k}$ vector in a specific direction in the plane perpendicular to the field until the Fermi energy was found with an accuracy of 1 μRy, for each of the split bands. The areas were then obtained by numerical integration of $|\mathbf{k}_F|^2$ around an orbit with a step in angle of 2.5°. The cyclotron-orbit mass was calculated using the integral

$$\int_0^{2\pi} \frac{|\mathbf{k}_F|}{\hat{\mathbf{k}}_F \cdot \mathbf{v}_\perp} d\phi = \frac{2\pi m_c^*}{\hbar m_0},$$

where m_0 is the free-electron mass. $\hat{\mathbf{k}}_F \cdot \mathbf{v}_\perp$ was approximated with

$$\frac{E(\mathbf{k}_F + \Delta\mathbf{k}) - E(\mathbf{k}_F - \Delta\mathbf{k})}{2|\Delta\mathbf{k}|},$$

with $\Delta\mathbf{k} = 10^{-4}(2\pi/a)$, where a is the lattice constant, in the same direction as $\mathbf{k}_F$. The split areas were then used to calculate R according to Eq. (1). The effective masses can then be used to calculate g_c from Eq. (2).

The routine was tested with respect to symmetric properties and linearity with applied field for small fields (up to 20 T). The calculations were performed for the fcc structure and a lattice constant of 3.89 Å for Pd and 3.92 Å for Pt. Complete self-consistent calculations were carried out for several different field directions in the symmetry planes with a field of 10 T. The sizes of the cyclotron-orbit areas compared to the experimental ones agree within 10%, except for the small X pockets.

With a field of 10 T in the [100] direction, the calculated spin magnetization in Pd is $0.0092\mu_B$ per atom, and the orbital magnetic moment is $0.0016\mu_B$ per atom, giving a total susceptibility of 8.6×10^{-4}. For Pt the corresponding moments are $0.0025\mu_B$ per atom and $0.0011\mu_B$ per atom, and the susceptibility is 2.8×10^{-4}. Compared to the experimental low-temperature values of 10.5×10^{-4} and 3.0×10^{-4}, respectively, this must be called good agreement. The Pauli susceptibility, $\mu_0\mu_B^2 D(E_F)$, where $D(E_F)$ is the density of states at the Fermi level, is 1.1×10^{-4} in Pd and 8.0×10^{-5} in Pt.

It is interesting to note that the enhancement of the calculated susceptibility does not only come from exchange-correlation effects on the spin magnetization, but also to a large extent from the spin-orbit coupling. The orbital moment contributes 15% to the total magnetization in Pd and 30% in Pt. In both metals the spin susceptibility shows an anisotropic behavior of approximately 2%. This anisotropy could be an effect of the numerical procedure, but appeared too systematic to be a calculational error, with the largest value of the susceptibility in the [100] direction, and smaller values in [110] and [111].

The calculated curve for R on the $\Gamma 6$ surface in Pd is shown in Fig. 1, together with the experimentally determined anisotropy [3]. Figure 2 presents calculated and experimental [3] R values for the $\alpha 5$ orbit in Pd. Comparison with Ohlsén and Calais [11], where spin-orbit interaction is included but no exchange-correlation effects are enhancing the Zeeman splitting, shows that the improvement in agreement with respect to anisotropic behavior, when comparing to experiment, is small but significant. As for all studied orbits, the Zeeman splitting is several times larger than the values presented in Ref. [11]. Regarding the g_c factor on the $X4$ pocket in Pd, the differences in anisotropic behavior are larger (Fig. 3).

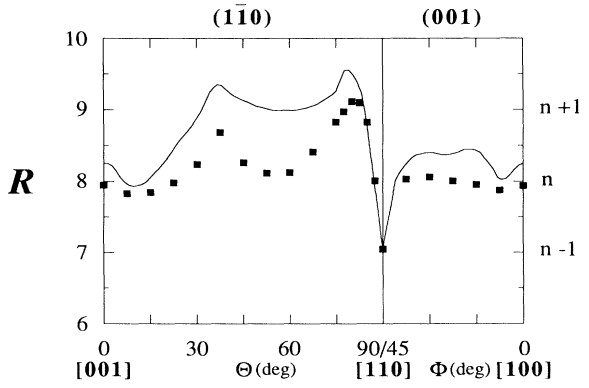

FIG. 1. Calculated values of R (solid squares) as a function of magnetic-field direction with the field in the symmetry planes on the $\Gamma 6$ Fermi-surface sheet in Pd. The experimentally determined anisotropy from Ref. [3] is also displayed (solid line). In the plot the arbitrary integer in the experimental result, indicated on the right scale, has been chosen as 8.

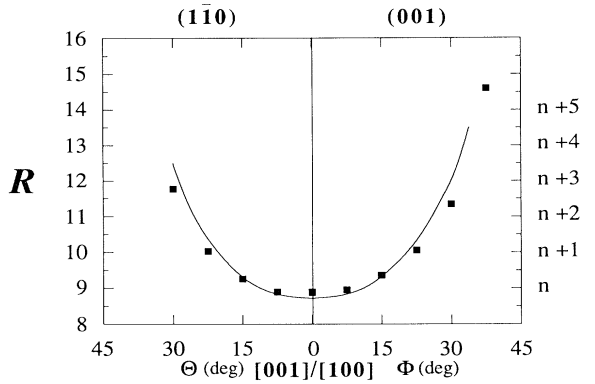

FIG. 2. R from calculations (solid squares) and experiments [3] (solid line) for the $\alpha 5$ orbit in Pd. The left panel shows a (1$\bar{1}$0) plane and the right one a (001) plane. The experimental data are displayed with the arbitrary integer n equal to 9.

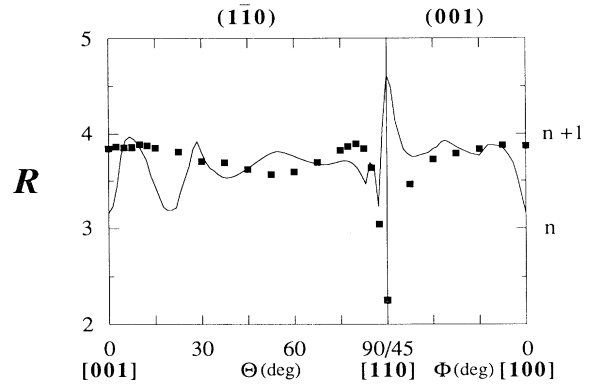

FIG. 4. Same as Fig. 1, but for platinum with $n=3$. Experimental results are from Ref. [6].

In the present calculations the value of g_c in [001] is larger than around the "waist" of the pocket, in contrast to Ref. [11], indicating that the exchange-correlation enhancement of the Zeeman splitting is strongly anisotropic, with a larger effect near [001] than in the (001) plane. This is in line with experimental studies, in which a small amount of Ni in Pd has been used in order to increase the exchange-correlation effects [18]. The reason for displaying g_c rather than R for $X4$ pockets is that this change in anisotropic behavior with respect to Ref. [11] is easier to observe in the curves showing g_c.

In Pt discrepancies are larger. From Fig. 4, displaying R on the $\Gamma 6$ surface, it is obvious that the model cannot reproduce the extremely rapid variations of R in the vicinity of [001] and [110]. There is also a discrepancy regarding the value in the [110] direction, where the calculations show a minimum—as both theory and experiment indicate in Pd—while the experimental interpretation gives a maximum. For the α orbit, displayed in Fig. 5, the agreement between theory and experiment is better. The calculated g_c factor on the X pocket hole in Pt, shown in Fig. 6, is in general too small. However, the agreement with experiment [7] with respect to anisotropic behavior is better than in Ref. [11]. The differences between theory and experiment are larger on the X pockets than on the other Fermi-surface sheets. This may be because the calculated cross-sectional area of this tiny Fermi-surface sheet is twice the size of the experimental one, and because the cyclotron orbits on the X pockets cross the Brillouin-zone boundary.

For the large Fermi-surface sheets in Pd and Pt the results presented in this work show very good agreement with experiment. This clearly demonstrates that exchange, correlation, and relativistic effects must be included when studying the eigenstates of conduction electrons in external magnetic fields, and that the magnetic field must be included in a self-consistent way. It is also shown that the LMTO method in the scalar relativistic approximation with the spin-orbit coupling in a separate term, the introduction of the field through the Zeeman

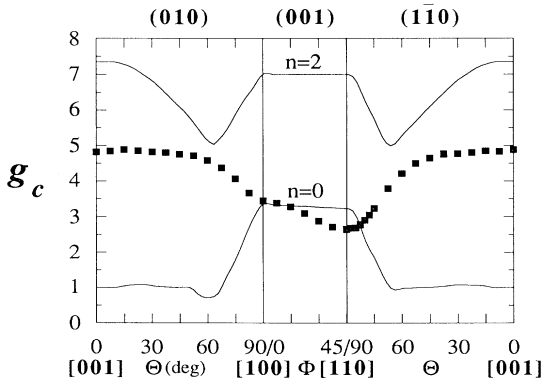

FIG. 3. Calculated (solid squares) and experimental [4] (solid line) g_c factor on the $X4$ pocket in Pd. In the derivation of the calculated values an electron-phonon coupling constant of 1.9 has been used. Two alternatives for the experimental values are presented, with the arbitrary integer equal to 0 or 2.

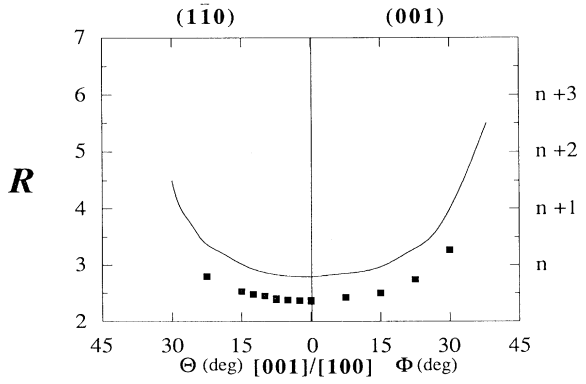

FIG. 5. Same as Fig. 2, but for platinum, and $n=3$. Experimental results are from Ref. [6].

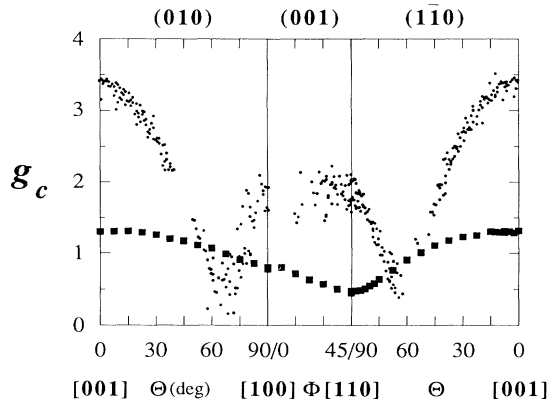

FIG. 6. Calculated (solid squares) and experimental [7] (solid circles) g_c factor on the $X4$ pocket in Pt. The electron-phonon coupling constant used for the calculated values is 1.5. The experimental values are presented with the arbitrary integer equal to 0.

term, the LSDA with spherically averaged densities, and the parametrized exchange-correlation potential from von Barth and Hedin [16] serves as a useful tool for calculating the electronic structure of metals in external magnetic fields.

It is worth noting that this model, with the magnetic field omitted, has given very good results for itinerant ferromagnets (see, e.g., Ref. [17]), although the parametrization of the exchange-correlation potential is most accurate in the paramagnetic region [16]. This suggests that the approach described in this paper might be useful across the border to ferromagnetism, in order to study, e.g., magnetocrystalline anisotropy, magnetostriction, and metamagnetic transitions.

Discussions with Sven Hörnfeldt, Per Nordblad, Lars Nordborg, Lars Nordström, and Håkan Ohlsén are gratefully acknowledged.

[1] J. M. Perz and D. Shoenberg, J. Low Temp. Phys. **25**, 275 (1976); B. Knecht, J. Low Temp. Phys. **21**, 619 (1975); M. Springford, I. M. Templeton, and P. T. Coleridge, J. Low Temp. Phys. **53**, 563 (1983).
[2] H. Ohlsén, P. Gustafsson, and L. Nordborg, J. Phys. F **16**, L79 (1986).
[3] H. Ohlsén, P. Gustafsson, L. Nordborg, and S. P. Hörnfeldt, Phys. Rev. B **29**, 3022 (1984).
[4] H. Ohlsén, P. Gustafsson, and L. Nordborg, J. Phys. F **16**, 1681 (1986).
[5] P. Gustafsson, H. Ohlsén, and L. Nordborg, J. Phys. F **17**, 117 (1987); A. Hjelm, L. Nordborg, and H. Ohlsén, Phys. Rev. B **41**, 7446 (1990).
[6] P. Gustafsson, H. Ohlsén, and L. Nordborg, Phys. Rev. B **33**, 3749 (1986).
[7] A. Hjelm, H. Ohlsén, and L. Nordborg, Phys. Rev. B **36**, 4647 (1987).
[8] D. L. Randles, Proc. R. Soc. London A **331**, 85 (1972); P. T. Coleridge, G. B. Scott, and I. M. Templeton, Can. J. Phys. **50**, 1999 (1972); W. M. Bibby and D. Shoenberg, J. Low Temp. Phys. **34**, 659 (1979); G. W. Crabtree, L. R. Windmiller, and J. B. Ketterson, J. Low Temp. Phys. **20**, 655 (1975); **26**, 755 (1977); H. Alles, R. J. Higgins, and D. H. Lowndes, Phys. Rev. B **12**, 1304 (1975).
[9] A. H. MacDonald, J. Phys. F **12**, 2579 (1982).
[10] T. Jarlborg and A. J. Freeman, Phys. Rev. B **23**, 3577 (1981).
[11] H. Ohlsén and J.-L. Calais, Phys. Rev. B **35**, 7914 (1987).
[12] O. Eriksson, H. Ohlsén, and J.-L. Calais, Phys. Rev. B **40**, 5961 (1989); G. E. Grechnev, N. V. Savchenko, I. V. Svechkarev, M. J. G. Lee, and J. M. Perz, Phys. Rev. B **39**, 9865 (1989).
[13] Anders Hjelm and Jean-Louis Calais (to be published).
[14] S. Engelsberg and G. Simpson, Phys. Rev. B **2**, 1657 (1970).
[15] H. Skriver, *The LMTO Method* (Springer-Verlag, Berlin, 1984).
[16] U. von Barth and L. Hedin, J. Phys. C **5**, 1629 (1972).
[17] Olle Eriksson, Ph.D. thesis, Uppsala University [Acta Univ. Uppsala **203** (1989)].
[18] H. Ohlsén and L. Nordborg, J. Phys. F **17**, 885 (1987).